

# 1

## Introduction

Interferometric synthetic aperture radar (InSAR) is an active remote sensing method that uses repeated radar scans of the Earth's solid surface to measure relative deformation at cm precision over a wide swath. This method has revolutionized our understanding of the earthquake cycle, volcanic eruptions, landslides, glacier flow, ice grounding lines, ground fluid injection/withdrawal, underground nuclear tests, and many other applications that require high spatial resolution measurements of ground deformation (Biggs and Wright, 2020; Joughin et al., 2010; Galloway and Hoffmann, 2007; Wei, 2017). The most recent generation of InSAR satellites has transformed the method from investigating 10s to 100s of synthetic aperture radar (SAR) images to processing 1 000s and 10 000s of images using a wide range of computer facilities. This transformation was largely driven by the Sentinel-1 mission, which was designed for InSAR time series analysis. There are a number of excellent review papers on this topic ranging from InSAR overviews (e.g., Massonnet and Feigl (1998); Bürgmann et al. (2000)) to detailed mathematical descriptions of the measurement and associated errors (Rosen et al. (2000); Simons and Rosen (2007, 2015); Franceschetti and Lanari (2018)).

The focus of this book is to provide the basic physical principles of the method as well as the mathematical model and algorithms used in InSAR processing. These algorithms are implemented in a computer software package called GMTSAR – an open-source (GNU General Public License) InSAR processing system designed for users familiar with generic mapping tools (GMT – (Wessel et al., 2019)). Although the book refers to this particular software, it is also relevant to other modern InSAR processing systems (e.g., ISCE – (Rosen et al., 2012), GAMMA – (Wegmüller et al., 2016), SNAP). This book has been developed over the past 25 years from a Space Geodesy class at Scripps Institution of Oceanography as well as GMTSAR short courses at UNAVCO and EarthScope. Each chapter has a set of problems and solutions to highlight the important concepts. In addition, we will answer 16 basic questions related to InSAR, including:

1. What are the six main categories of satellite remote sensing and why is active remote sensing at microwave wavelengths (2.5 cm–25 cm) best for measuring Earth deformation? (Section 1.2)
2. Why are SAR antennas typically 10 m long in the along-track direction and 1–2 m wide in the cross-track direction? (Section 2.3)
3. What factors control the spatial resolution of a SAR image? (Sections 2.4)
4. What factors limit the width of a SAR swath? (Section 2.5)
5. What are the typical orbital characteristics (e.g., altitude, speed, repeat cycle) of an InSAR satellite and why? (Section 3.2)
6. A C-band SAR operates at a 5 GHz carrier frequency. Why can the full-resolution radar data be recorded at a much lower rate of perhaps 15 MHz? (Section 4.2)
7. How is the raw SAR data focused by a computer to obtain a high spatial resolution image of amplitude and phase? (Chapter 4)
8. What orbit accuracy is needed to achieve an optimally focused SAR image? (Sections 4.5 and 4.6)
9. How is an interferogram constructed from repeated SAR images and what are the main contributions to the phase? (Sections 5.1 and 5.2)
10. How close in space does the repeat orbit need to match the reference orbit to achieve high correlation and good phase recovery? (Section 5.5)
11. How does decorrelation depend on radar wavelength and surface properties? (Section 6.2)
12. What is the best way to detect phase unwrapping errors? (Section 7.5)
13. What are the three main methods for achieving wide swath InSAR? (Chapter 8)
14. What are the main sources of error in most interferograms? (Chapter 9)
15. How can one construct an InSAR time series using existing freely open data sets? (Chapter 10)
16. How can a scalar InSAR time series be integrated with a vector GNSS time series? (Chapter 11)

The processing details associated with the last two questions are addressed in a companion book entitled – *Satellite Radar Interferometry: Application – GMTSAR*. This book mainly covers the theoretical aspects of InSAR. We will begin with a very brief overview of satellite remote sensing to answer the first question.

## 1.1 Essential Ingredients for Satellite Remote Sensing

Satellite remote sensing of the surface of the Earth relies on four essential ingredients:

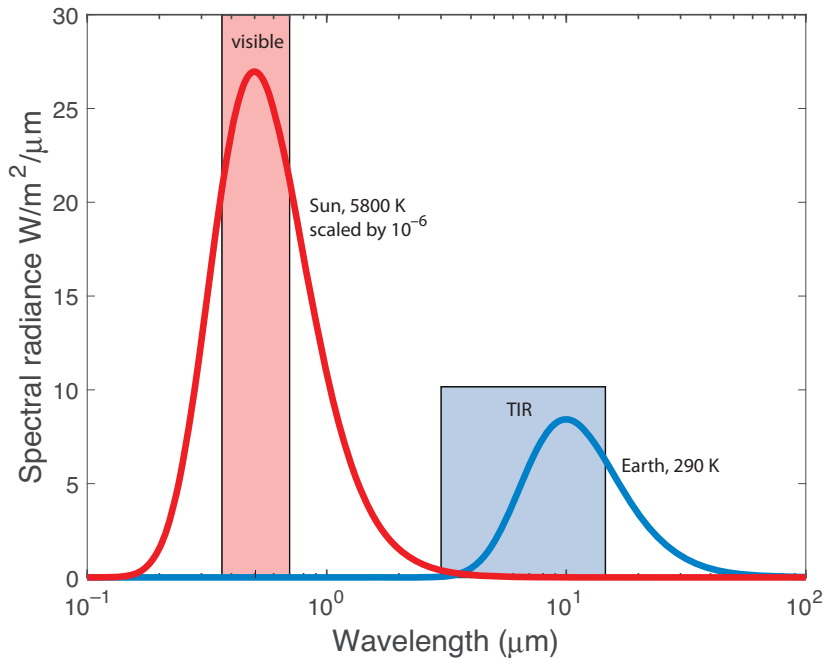


Figure 1.1 Blackbody radiation curves for a temperature of 5 800 K corresponding to the Sun and 290 K roughly corresponding to the Earth. The peak in the solar radiation (scaled by  $10^{-6}$ ) is centered on the visible part of the spectrum between 400 and 800 nanometers. The peak in the Earth's thermal radiation occurs in the thermal infrared (TIR) between 3 and 15 micrometers.

First, there must be a source of electromagnetic (EM) radiation. This could be passive radiation (Figure 1.1) from reflected sunlight, which peaks in the visible part of the spectrum (red curve), or passive radiation from the Earth's thermal emissions, which peaks in the thermal infrared (TIR) part of the spectrum (blue curve). An alternate radiation source is for the satellite to illuminate the Earth using an active sensor. While this requires significant power to generate the EM signal, the amplitude and phase of the source can be well controlled so one can measure the round-trip travel time of the pulse.

Second, the EM radiation must be able to pass through the Earth's atmosphere. As shown in Figure 1.2, there are three main windows in the visible (shaded red), thermal infrared (TIR; shaded blue), and microwave region (shaded green).

Third, there needs to be a satellite in space to collect the EM signals, digitize the signals, and transmit the data back to Earth. The satellite must be in orbit around the Earth so the inward force of gravity must be equal to the outward centrifugal force. A variety of possible orbits are discussed in Chapter 3. One can tune the orbit and platform characteristics to vary altitude, speed, revisit time, phase of the orbit

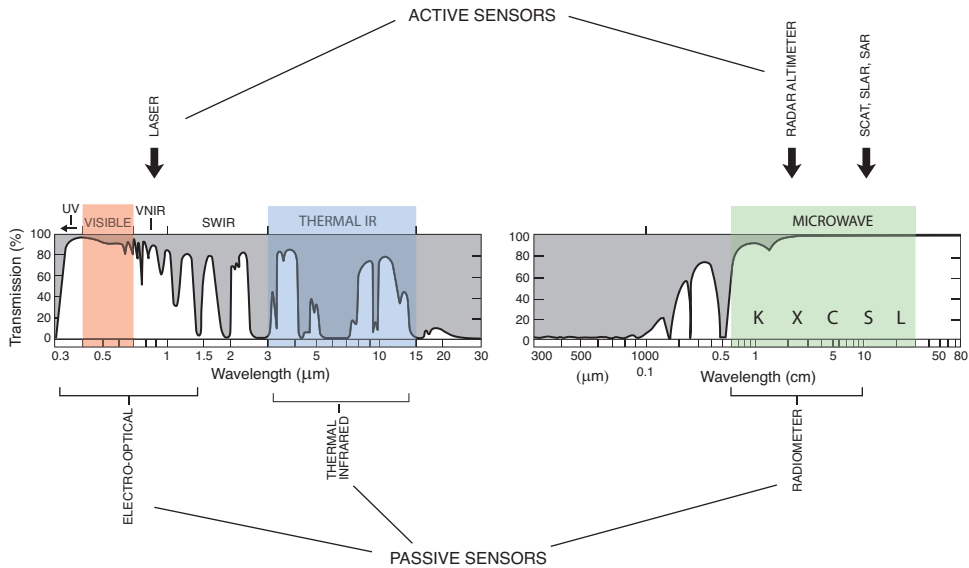


Figure 1.2 Percent transmission of EM waves through the Earth's atmosphere as a function of wavelength. There are three main windows where the atmosphere is mostly transparent. They are the visible (shaded red) centered at 0.5 micrometer, the TIR (shaded blue) centered at 8 micrometers with prominent windows at 3.5 and 10 micrometers, and the microwave (shaded green) at wavelengths between 0.6 cm and 30 cm. Note that EM waves at wavelengths greater than about 30 cm are strongly distorted and reflected by the ionosphere. The microwave region has bands noted by letters. The most common bands for radar interferometry are X, C, S, and L. The K-band is mainly used for radar altimetry and microwave radiometry.

plane with respect to solar illumination or lunar/solar tides, and platform orientation (yaw, pitch, and roll).

Fourth, there must be a computer and software (e.g., GMTSAR) to ingest the downlinked imagery/orbital information and construct maps of surface reflectance and deformation.

## 1.2 Main Categories of Satellite Remote Sensing

Based on these constraints, there are roughly six possible categories of Earth remote sensing instruments (i.e., three atmospheric windows and two modes – passive or active). These categories include:

The first type of passive sensor is an electro-optical instrument that operates in the visible part of the spectrum and uses cameras to construct imagery. A typical sensor is LANDSAT-7. The satellite was placed into a Sun-synchronous orbit having an inclination of 98.2 degrees and an altitude of 705 km. This seventh

LANDSAT had eight bands comprising six bands in the visible and near infrared with 30 m spatial resolution, a thermal infrared band with 60 m spatial resolution, and a panchromatic band with 15 m spatial resolution. These electro-optical sensors are usually placed into a Sun-synchronous orbit to provide relatively constant Sun illumination for each ascending (or descending) overflight. Very high spatial resolution optical sensors can measure sharp horizontal variations in surface deformation at a precision of about one tenth of a pixel size using cross-correlation methods on repeated images and these data are highly complementary to deformation measurements with InSAR (e.g., Avouac et al. (2006); Milliner et al. (2015)).

The second type of passive sensor is a TIR camera using the atmospheric window between 8 and 15 micrometers. The TIR camera measures thermal emissions from land or ocean surface, which can be used to infer surface temperature (e.g., McClain et al. (1985); Donlon et al. (2012)). These TIR cameras do not need to be in Sun-synchronous orbits and the acquisitions are designed to avoid specular reflections of solar radiation.

The third type of passive sensor is a microwave radiometer. This instrument uses the highly transparent window in the microwave part of the EM spectrum (1 cm–30 cm) to measure thermal emissions from the land (e.g., Reichle et al. (2007)) or ocean (e.g., Chelton and Wentz (2005)). Since they operate at wavelengths much longer than the  $\sim 10$  micrometer peak in the blackbody radian spectrum from the Earth at 290 K, they must stare at the surface for a relatively long time ( $\sim 0.1$  s) to gather enough independent looks to achieve an accurate measurement of temperature. Moreover, since they operate at this relatively long wavelength  $\lambda$ , a large antenna diameter  $D$  is needed to achieve a useful angular resolution  $\theta_a$ . In Chapter 2, we develop the Fraunhofer diffraction resolution  $\sin(\theta_a) = 1.22 \lambda/D$  to illustrate the pronounced resolution differences between short-wavelength optical systems ( $\lambda = \sim 0.5$  micrometers) and longer wavelength microwave systems ( $\lambda = \sim 50$  mm).

The fourth sensor is an active laser altimeter that can be used to measure the topography of a wide range of surfaces, including ocean, ice, land, vegetation, and buildings. The atmosphere is sometimes opaque over the visible part of the spectrum because of clouds. The lidar can measure distances very accurately by sending a sharp pulse of light and measuring the two-way travel time of the reflected pulse. Monitoring changes in ocean ice and continent ice thickness are two of the most important applications of this method (Markus et al. (2017)).

The fifth sensor is an active radar altimeter that is best for measuring the topography of the ocean surface and changes in sea surface height due to a wide range of oceanographic processes (Fu and Cazenave (2000)). As we will discuss in

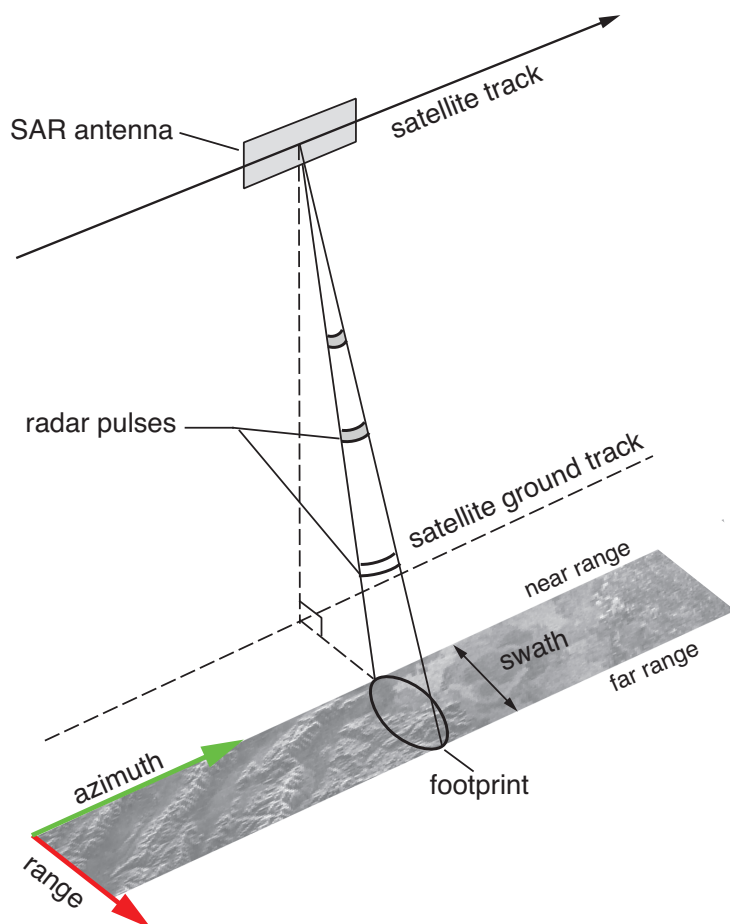


Figure 1.3 Schematic diagram of a SAR satellite in orbit. The SAR antenna has its long axis in the flight direction (also called the *azimuth* direction) and the short axis in the *range* direction. The radar sends pulses to one side of the *ground track* that illuminate the Earth over a large elliptical footprint. The reflected energy returns to the radar where it is recorded as a function of *fast time* in the range direction and *slow time* in the azimuth direction.

Chapter 2, the beam-limited footprint of a radar altimeter is 10s of km in diameter. To reduce the diameter of the footprint, the radar emits a sharp pulse having a spherical wavefront. The radar measures the two-way travel time of the leading edge of the pulse, which corresponds to the closest reflector from the satellite. Over the ocean this is also the *nadir* point as well as the zero-Doppler shift point. In practice, it is difficult to send a very sharp radar pulse so the radar emits a rather long frequency-modulated chirp that reflects from the ocean and returns to the sensor.

A sharp pulse is formed after reception by deconvolving the return chirp with a replica of the outgoing chirp.

The sixth sensor is an active radar that sends pulses of microwave energy to the side of the sub-satellite ground track (e.g., Curlander and McDonough (1991)) as shown in Figure 1.3. Like a radar altimeter, these pulses have broad spherical wavefronts that reflect off a large ellipsoidal *footprint* forming a wide *swath*. The first reflections come from the *near-range* edge of the swath. The pulse sweeps across the swath to the *far-range* edge of the swath.

The data collected by this side-looking radar have very poor spatial resolution related to the large size of the footprint. Chapters 2–4, we will describe how these data are focused first in the range direction and then in the azimuth direction using a synthetic aperture method (SAR). This is a good place to note that the raw SAR data come as a 2-D array of numbers. The rows of the file correspond to the *range* direction marked by the red arrow in Figure 1.3. The columns in the file correspond to the along-track direction of the satellite, which is also called *azimuth* marked by the green arrow in Figure 1.3. The data are equally spaced in time in both dimensions. The time spacing in the range direction is  $1/\text{range sampling rate}$ . If the range cells are  $\Delta\rho = 5$  meters, then the range sampling rate  $\Delta t = c/(2 * \Delta\rho) = 30$  MHz, where  $c$  is the speed of light. This dimension is also called *fast time* because of the high sampling rate. The sampling rate in the azimuth direction, also called the *pulse repetition frequency* (PRF) is much lower at  $\sim 1\,500$  Hz; this dimension is called *slow time*. In Chapter 2, we will discuss how these sampling rates are related to the resolution of the SAR image as well as the velocity of the spacecraft and the length of the antenna.